Best
Available
Copy

AD-778 949

MEASURED N2O-N2 ABSORPTION AT FIVE DF
LASER FREQUENCIES

F. S. Mills, et al

Ohio State University

RADC-TR-74-89
Technical Report
March 1974

MEASURED N_2O-N_2 ABSORPTION
AT FIVE DF LASER FREQUENCIES

The Ohio State University

ElectroScience Laboratory

Department of Electrical Engineering
Columbus, Ohio 43212

DDC
RECEIVED
MAY 16 1974
C

Approved for public release;
distribution unlimited.

Rome Air Development Center
Air Force Systems Command
Griffiss Air Force Base, New York

SECURITY CLASSIFICATION OF THIS PAGE *(When Data Entered)*

REPORT DOCUMENTATION PAGE		READ INSTRUCTIONS BEFORE COMPLETING FORM
1. REPORT NUMBER RADC-TR-74-89	2. GOVT ACCESSION NO.	3. RECIPIENT'S CATALOG NUMBER
4. TITLE *(and Subtitle)* Measured N_2O-N_2 Absorption at Five DF Laser Frequencies		5. TYPE OF REPORT & PERIOD COVERED Interim
		6. PERFORMING ORG. REPORT NUMBER ESL 3271-9
7. AUTHOR(s) F. S. Mills R. K. Long		8. CONTRACT OR GRANT NUMBER(s) F30602-72-C-0016
9. PERFORMING ORGANIZATION NAME AND ADDRESS Ohio State University Electroscience Laboratory		10. PROGRAM ELEMENT, PROJECT, TASK AREA & WORK UNIT NUMBERS PE 62301E Project 12790502
11. CONTROLLING OFFICE NAME AND ADDRESS Advanced Research Projects Agency 1400 Wilson Blvd. Arlington, VA 22209		12. REPORT DATE March 74
		13. NUMBER OF PAGES 34
14. MONITORING AGENCY NAME & ADDRESS*(if different from Controlling Office)* Rome Air Development Center RADC/OCSE Griffiss AFB NY 13441		15. SECURITY CLASS. *(of this report)* Unclassified
		15a. DECLASSIFICATION/DOWNGRADING SCHEDULE N/A

16. DISTRIBUTION STATEMENT *(of this Report)*

Approved for public release; distribution unlimited.

17. DISTRIBUTION STATEMENT *(of the abstract entered in Block 20, if different from Report)*

Same

18. SUPPLEMENTARY NOTES

Monitored by   James W. Cusack, RADC/OCSE
               Griffiss AFB NY 13441

DDC
RECEIVED
MAY 16 1974
C

19. KEY WORDS *(Continue on reverse side if necessary and identify by block number)*

DF Laser   Molecular Absorption
Laser Propagation
Atmosphere   Reproduced by
Nitrous Oxide   NATIONAL TECHNICAL
                         INFORMATION SERVICE
                         U S Department of Commerce
                         Springfield VA 22151

20. ABSTRACT *(Continue on reverse side if necessary and identify by block number)*

This report presents measurements of the absorption coefficients of N_2O-N_2 samples at five DF laser wavelengths (3-2 P6, P7, P8 and 2-1 P10, P11). A small grating-tunable pulsed DF laser was used in conjunction with a multi-traversal absorption cell having a path length for these experiments of 0.732 km. The results are compared with previously available experimental results and with calculated values.

DD FORM 1473   EDITION OF 1 NOV 65 IS OBSOLETE
1 JAN 73

SECURITY CLASSIFICATION OF THIS PAGE *(When Data Entered)*

MEASURED N_2O-N_2 ABSORPTION
AT FIVE DF LASER FREQUENCIES

F. S. Mills
R. K. Long

Principal Investigator: Dr. Ronald K. Long
Phone: 614 422-6077

Project Engineer: James W. Cusack
Phone: 315 330-3145

i a

FOREWORD

This report, Ohio State University Research Foundation Report Number 3271-9 (Ninth Quarterly Report), was prepared by The Ohio State University ElectroScience Laboratory, Department of Electrical Engineering at Columbus, Ohio. Research was conducted under Contract F 30602-72-C-0016. Mr. James W. Cusack, RADC (OCSE), of Rome Air Development Center, Griffiss Air Force Base, New York, is the Project Engineer.

This technical report has been reviewed and is approved.

James W. Cusack
RADC Project Engineer

ii

ABSTRACT

This report presents measurements of the absorption coefficients
of N_2O-N_2 samples at five DF laser wavelengths (3-2 P6, P7, P8 and
2-1 P10, P11). A small grating-tunable pulsed DF laser was used
in conjunction with a multi-traversal absorption cell having a
path length for these experiments of 0.732 km.

The results are compared with previously available experimental
results and with calculated values.

CONTENTS

I. INTRODUCTION

Recent calculations [1], reproduced here as Table I, have predicted that the sea level absorption coefficients for a representative list of 30 DF lines of the 3-2, 2-1, and 1-0 vibrational bands are in the range .022 to .268 km^{-1} for a mid-latitude summer atmospheric model. This model assumes 76% relative humidity at 70°F, 0.28 ppm N_2O, 1.6 ppm CH_4, 0.075 ppm CO, and 330 ppm CO_2 [2].

The purpose of the present work was to experimentally verify, for certain DF lines, that part of the predicted coefficient which is attributable to N_2O absorption. From Table I we see that this fraction is, for the 3-2 P6, P7, and P8 lines, 7%, 55%, and 32% respectively, whereas for the 2-1 P10 and P11 the fraction is 65% and 27% respectively.

Assuming that the calculations are in error by no more than ± 100 percent, it is not possible to measure the N_2O-N_2 absorption coefficients with acceptable accuracy using a one kilometer absorption cell unless the absorber amounts are increased above the normally assumed sea level concentrations. This is the approach which has been taken here. N_2O concentrations used were 10 to 1000 times normal atmospheric abundance (i.e., 2×10^{-3} to 2×10^{-1} torr for a total pressure of 760 torr). These N_2O concentrations are still quite low and it is shown that the results can be linearly extrapolated to normal N_2O abundance without distortion caused by self-broadening.

The calculated coefficients require accurate knowledge of the laser line frequencies. At the present time the 3-2 band frequencies are not known as accurately as the 2-1 and 1-0 band frequencies. In the present study it was possible to obtain an approximate value for the separation between the laser frequency and the nearest N_2O absorption line for the 3-2 P(7) and 2-1 P(10) DF lines from a measurement of the absorption coefficient versus total pressure for a fixed absorber concentration.

II. DESCRIPTION OF EXPERIMENT

A block diagram of the experiment is shown in Fig. 1.

The laser is a small pulsed type similar to one originally described by Ultee [3]. The laser tube is constructed of 7 mm id pyrex tubing with two transverse inlet ports and three outlet ports. Electrodes are made of 1/8" copper tubing. The active length is approximately twelve inches. Calcium fluoride brewster windows are employed and a separate flow of helium is introduced near each window to reduce formation of previously troublesome sulphur deposits. This flow is adjusted for 5 torr tube pressure with the other gases shut off. Gases used in the laser are helium, sulfur hexafluoride, oxygen, and deuterium. Active elements are SF_6 and D_2 which react in the electric discharge to produce DF. Helium is added as a heat sink and also probably promotes discharge stability. A small flow of oxygen helps to keep the tube walls clean.

1

TABLE I

Mid-Latitude Summer Sea Level Absorption Coefficients
Calculated from AFCRL Absorption Line-Data

Line	Iden	S*	N_2O	CH_4	CO_2	H_2O	H_2O Cont	N_2	Total
2445.41	3-2,12	c	2.519E-3	4.268E-9	1.042E-2	3.095E-5	2.85E-2	6.6E-2	1.075E-1
2471.29	3-2,11	c	4.087E-3	7.683E-8	3.713E-5	4.997E-3	2.52E-2	4.6E-2	8.032E-2
2496.77	3-2,10	c	8.055E-4	1.109E-5	5.381E-8	6.540E-4	2.27E-2	2.5E-2	4.917E-2
2500.43	2-1,13	b	7.635E-3	2.881E-6	2.735E-8	1.267E-4	2.22E-2	2.5E-2	5.496E-2
2521.81	3-2,9	c	4.511E-4	2.748E-6	2.094E-7	2.321E-4	2.05E-2	1.5E-2	3.619E-2
2527.42	2-1,12	b	8.387E-4	1.841E-5	1.814E-7	2.539E-4	2.00E-2	1.4E-2	3.511E-2
2546.42	3-2,8	c	1.399E-2	1.833E-3	1.196E-7	1.347E-3	1.86E-2	8.0E-3	4.377E-2
2553.97	2-1,11	b	9.655E-3	7.757E-5	1.035E-7	5.113E-4	1.82E-2	7.1E-3	3.554E-2
2570.51	3-2,7	a	3.367E-2	3.174E-5	7.826E-8	4.783E-3	1.75E-2	5.0E-3	6.098E-2
2580.10	2-1,10	b	4.458E-2	2.618E-6	6.763E-8	2.684E-3	1.70E-2	3.6E-3	6.787E-2
2583.47	1-0,13	b	2.517E-2	5.008E-6	6.441E-8	3.580E-3	1.69E-2	3.45E-3	4.91 E-2
2594.25	3-2,6	c	1.954E-3	1.612E-5	5.553E-8	6.666E-3	1.68E-2	2.6E-3	2.804E-2
2605.80	2-1,9	b	5.362E-4	2.046E-4	4.792E-8	1.937E-2	1.68E-2	2.3E-3	3.921E-2
2611.14	1-0,12	b	9.147E-5	3.795E-6	4.432E-8	8.245E-3	1.70E-2	2.1E-3	2.744E-2
2617.44	3-2,5	c	1.170E-5	7.513E-5	4.174E-8	2.872E-3	1.72E-2	2.0E-3	2.216E-2
2631.06	2-1,8	b	1.229E-7	7.884E-4	3.591E-8	1.476E-2	1.78E-2	1.9E-3	3.525E-2
2638.39	1-0,11	b	1.271E-8	5.999E-4	3.327E-8	2.472E-1	1.82E-2	1.6E-3	2.676E-1
2655.85	2-1,7	b	1.103E-11	6.015E-4	2.805E-8	7.905E-2	1.93E-2		9.895E-2
2665.22	1-0,10	b	1.418E-11	1.975E-3	2.573E-8	1.512E-2	2.00E-2		3.709E-2
2680.17	2-1,6	b	2.291E-11	3.103E-4	2.260E-8	3.689E-2	2.12E-2		5.84 E-2
2691.61	1-0,9	b	3.647E-11	3.223E-3	2.057E-8	5.509E-2	2.20E-2		8.03 E-2
2703.99	2-1,5	b	7.099E-11	2.073E-6	1.867E-8	5.454E-3	2.30E-2		2.846E-2
2717.54	1-0,8	b	2.441E-9	2.335E-6	1.638E-8	8.986E-2	2.41E-2		1.14 E-1
2727.30	2-1,4	b	2.679E-8	1.475E-4	1.574E-8	4.248E-2	2.51E-2		6.773E-2
2743.00	1-0,7	b	4.321E-6	2.850E-4	1.414E-8	3.300E-2	2.69E-2		6.019E-2
2750.09	2-1,3	b	4.052E-5	8.969E-4	1.350E-8	1.255E-2	2.75E-2		4.099E-2
2767.97	1-0,6	b	1.029E-4	4.949E-3	1.206E-8	5.130E-2	3.08E-2		8.715E-2
2792.43	1-0,5	b	8.076E-4	6.103E-4	1.044E-8	3.732E-2	3.50E-2		7.374E-2
2816.38	1-0,4	b	1.158E-3	2.859E-3	9.144E-9	6.043E-2	4.00E-2		1.044E-1
2839.78	1-0,3	b	4.945E-7	7.241E-4	8.100E-9	5.749E-2	4.50E-2		1.032E-1

*Source of laser line data
a - Mills (OSU)
b - calculated from molecular constants (P.K.L. Yin, OSU Physics Dept.)
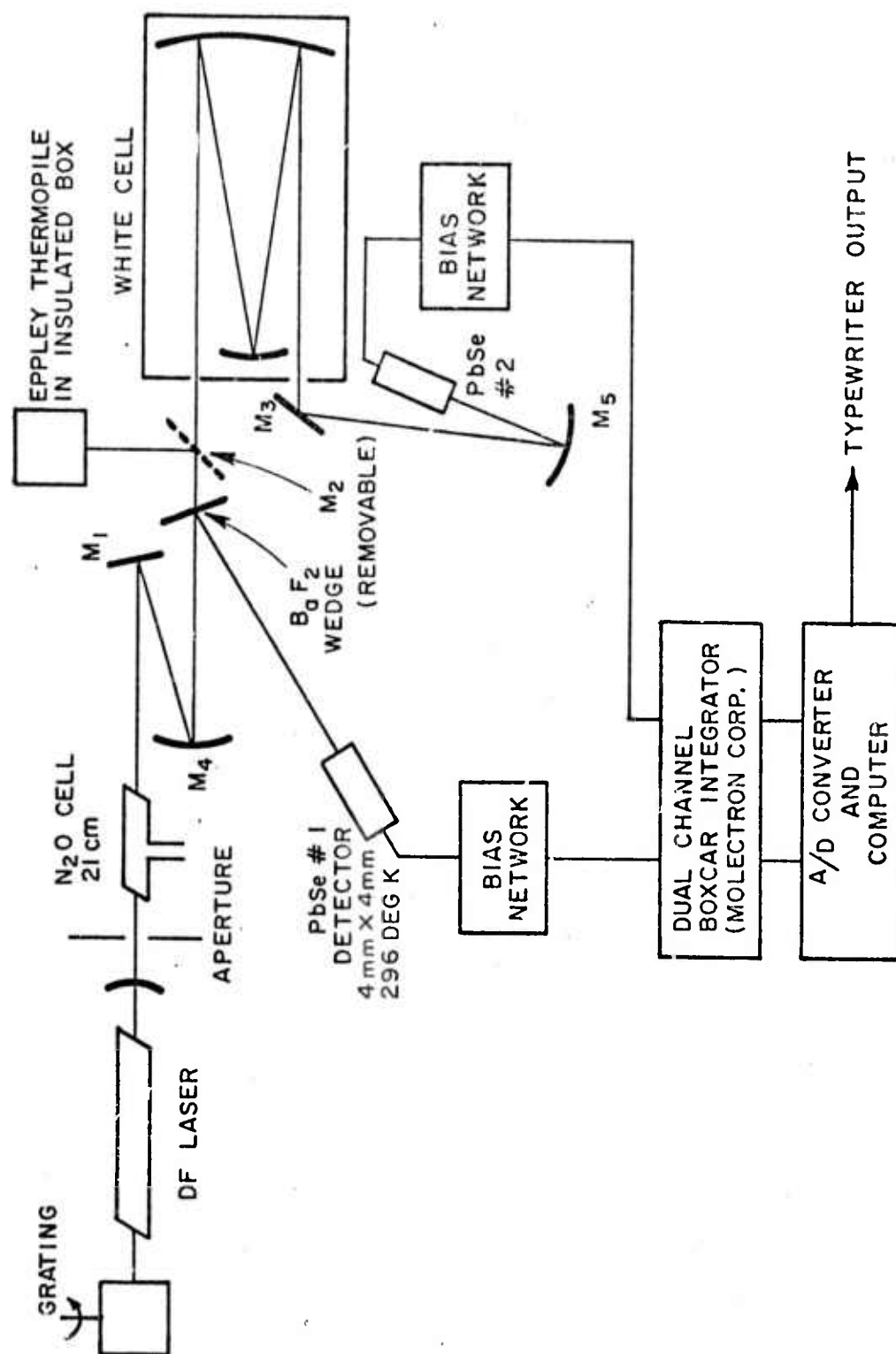c - Deutsch (7)

2

Fig. 1. Schematic diagram of DF laser absorption experiment.

A 15 cfm mechanical vacuum pump is used to maintain a discharge tube pressure of 15 torr and a flow rate sufficient to change the gas mixture in the tube between pulses. The optimum pressure varies somewhat according to the laser line which is oscillating. The laser discharge is created by discharging a 0.01 μfd capacitor which has been charged to 14 kv. The pulses are 2 microseconds long and occur at a rate of 36 pulses per second. The latter value is vacuum pump limited and determines the maximum average power which can be obtained.

The optical cavity consists of a 300 line/mm grating blazed at 3 μm and a 20 m radius of curvature Germanium mirror coated for greater than 80% reflectivity between 3 μm and 4 μm. The grating and mirror are separated by 121 cm. The mirror is mounted in a piezoelectric drive and a mechanical translation stage to provide cavity length adjustment. The grating mount, laser tube and mirror mount are all attached to a 5' x 1' x 3" limestone slab. This arrangement has proved to be quite stable. Figure 2 shows a photograph of the laser. The entire laser and power supply are placed in a standard electromagnetic shielded room in order to reduce interference with the remainder of the experimental electronics. The optical output is through a hole in the shield and the pulse trigger output required by the boxcar integrator is coupled out of the shielded room by a solid state optical isolator device.

The thirty lines listed in Table I are all observed with this laser. The average power output is approximately one milliwatt per line.

The 21 cm N_2O cell shown in Fig. 1 was used as an attenuator in a detector linearity calibration experiment which was performed prior to the N_2O-N_2 measurements. The details of this somewhat involved procedure are described in Appendix A. The on-line computer data recording program used the calibration data to correct the absorption coefficient measurements for detector non-linearities.

For each experimental run the multi-traversal cell was evacuated and the transmittance of the empty cell was measured. A certain pressure of a mixture of 10,000 ppm N_2O in N_2 (based on manufacturer's analysis) was then admitted to the cell followed by a dry nitrogen fill to 760 torr. Mixing fans were turned on for one hour. This gave a mixture at the highest N_2O concentration to be measured during that run. After the transmittance of that mixture was measured, the absorption cell was partially pumped out, the pressure measured, and the cell refilled to 760 torr with dry N_2. This procedure reduced the N_2O concentration by a known amount. The new sample was allowed to mix for one hour and its transmittance was measured. This procedure was repeated to obtain data at several N_2O concentrations. At the end of the day the cell was again evacuated and the transmittance measured. The entire process was repeated several times on different days for each laser line. All measurements were made at room temperature (72-74°F).
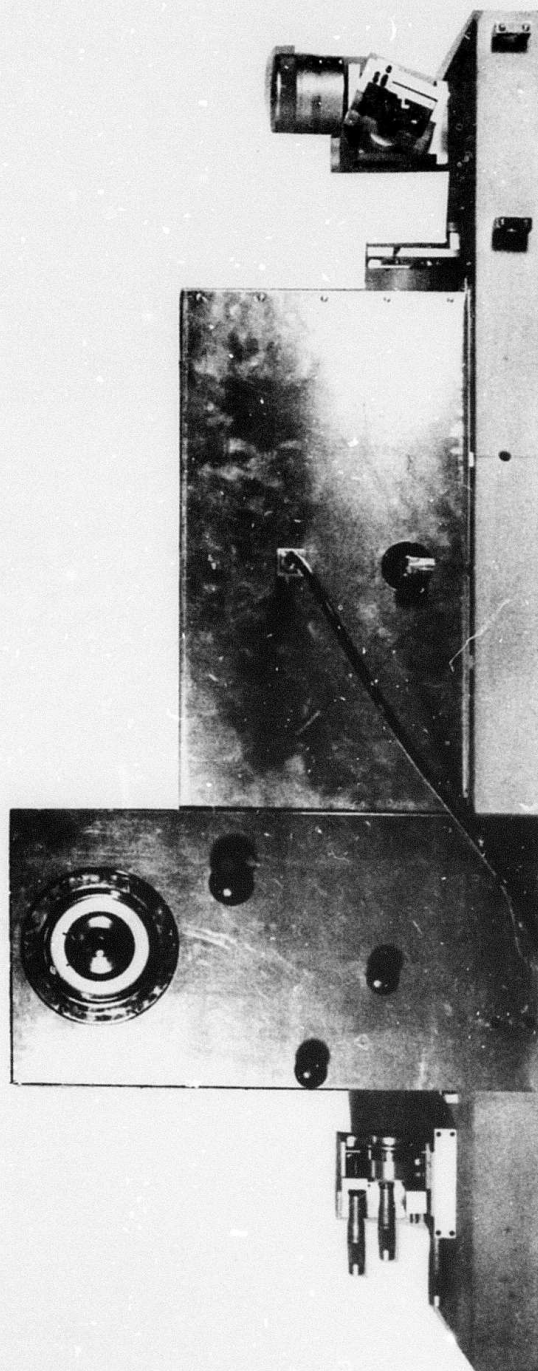
Fig. 2. The pulsed DF probe laser.

5

Although the laser was tunable from line to line, it was found that the desired repeatibility in transmittance (1%) could not be obtained unless the laser was left tuned to one line for the duration of a measurement run. This is presumably due to optical alignment difficulties associated with moving the grating.

III. RESULTS OF ABSORPTION COEFFICIENT MEASUREMENTS

Figures 3-7 show the measured absorption coefficients versus N_2O concentration for the five lines studied. In each case a least squares fit of the data to a straight line through the origin was made. The figures also show the predicted results using the AFCRL data tape [4] and the experimental results of Spencer [5] obtained from measurements on pure N_2O samples in a one meter cell.

Figures 8-11 show computed spectral plots [1] in the vicinity of the five laser lines. The plots are for one km path length, 760 torr total pressure, 72°F, and N_2O partial pressures as given on the figures. Note that in all five cases there is a near coincidence between an N_2O absorption line and a DF laser frequency. For this reason one might expect that errors in the N_2O or DF line frequencies would cause errors in the computed results. In fact the predictions and measurements are in quite good agreement although there is a greater discrepancy for those laser lines whose position is less well known, indicating that uncertainty in laser line position is a significant source of error in the calculations.

The excellent agreement of the measured values with those obtained by Spencer confirms the lack of significant self broadening effects in N_2O.

Assuming a natural N_2O abundance of 0.28 ppm [2], Table II gives the N_2O absorption coefficients for the five laser lines as extrapolated from the measured data. For comparison the calculated values from Table I are also given.

TABLE II

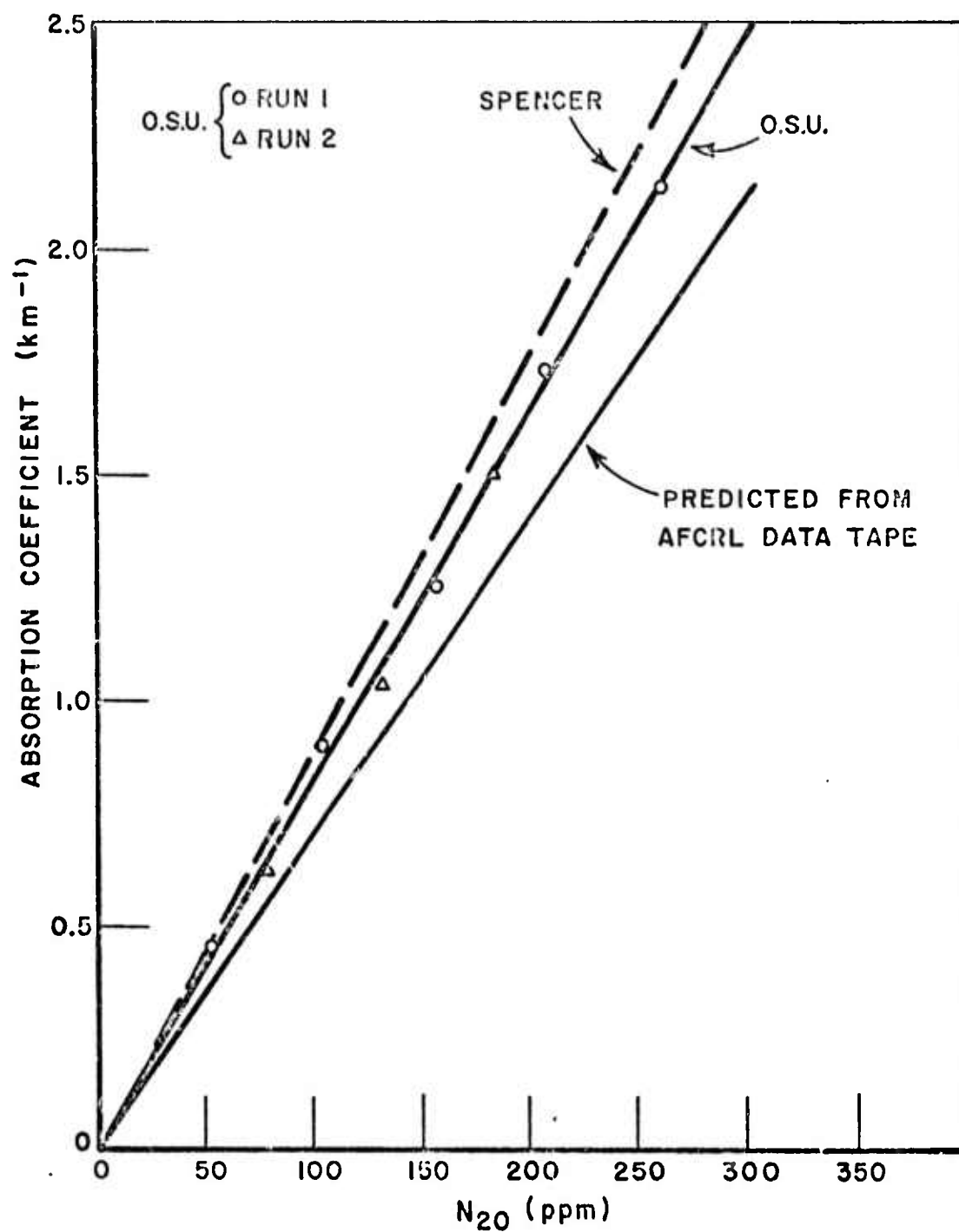| Iden	v (cm^{-1})	K_{exp}^{OSU} (km^{-1})	k_{calc} (km^{-1})	% DIFF $\left(\dfrac{CALC-EXP}{EXP}\right)$
3-2 P(7)	2570.51	.0373	.0337	-9.7
3-2 P(8)	2546.42	.0214	.0140	-35
2-1 P(10)	2580.10	.0453	.0446	-1.5
2-1 P(11)	2553.97	.00969	.00966	-.31
3-2 P(6)	2594.25	.00227	.00195	-14

6

Fig. 3. Measured N_2O-N_2 absorption coefficient for 3-2 P(6) line.
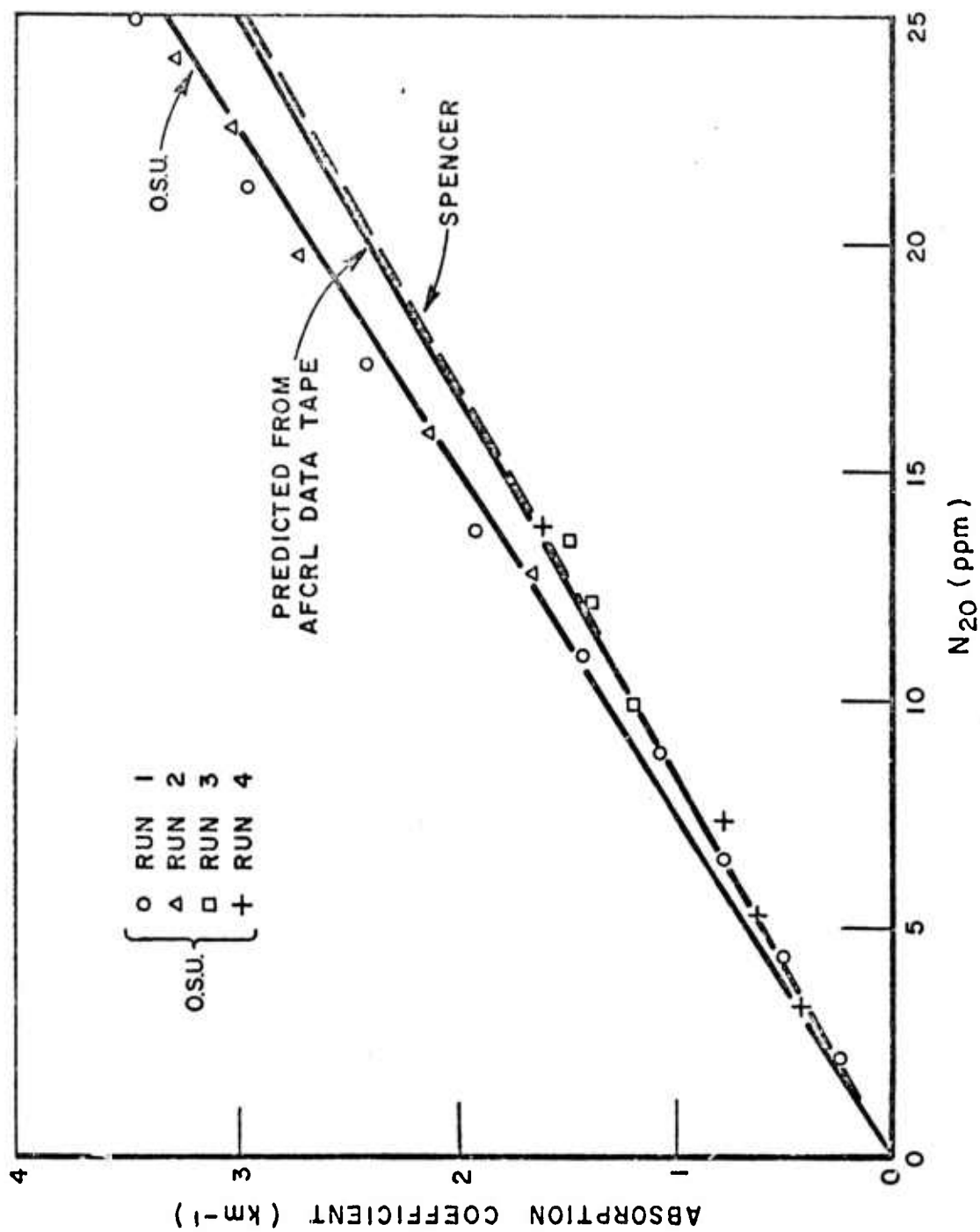
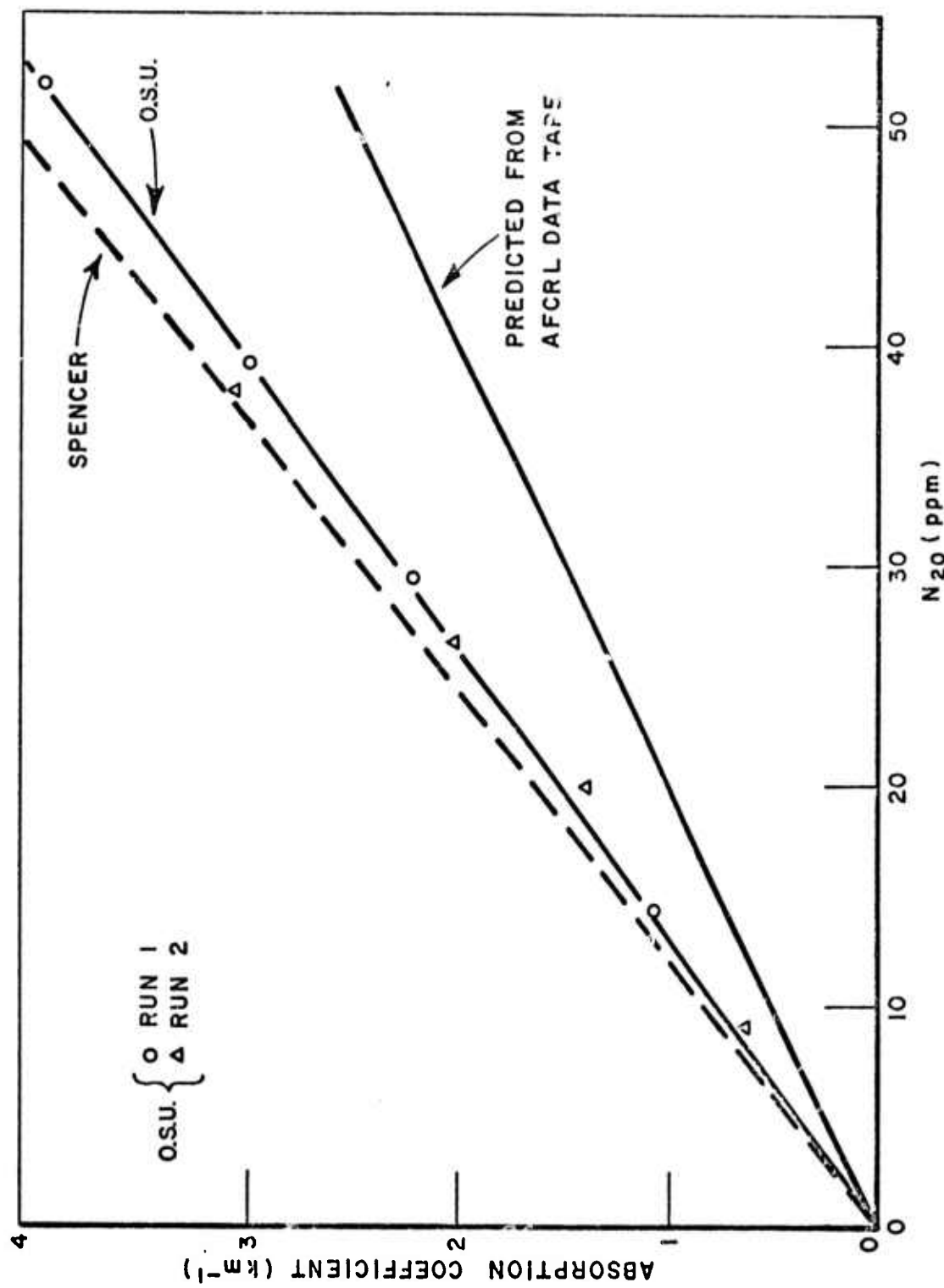Fig. 4. Measured N_2O-N_2 absorption coefficient for 3-2 P(7) line.

8

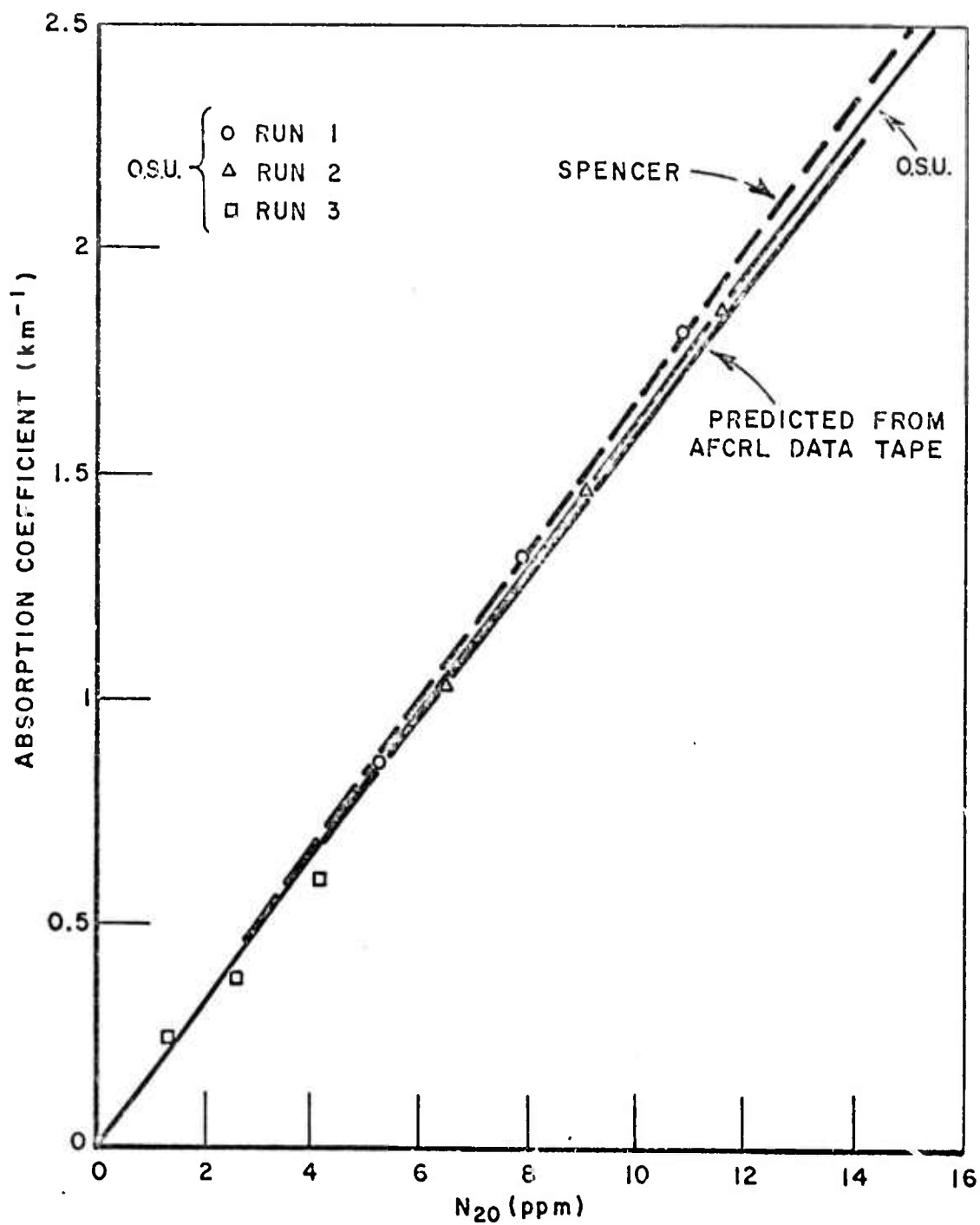Fig. 5. Measured N_2O-N_2 absorption coefficient for 3-2 P(8) line.

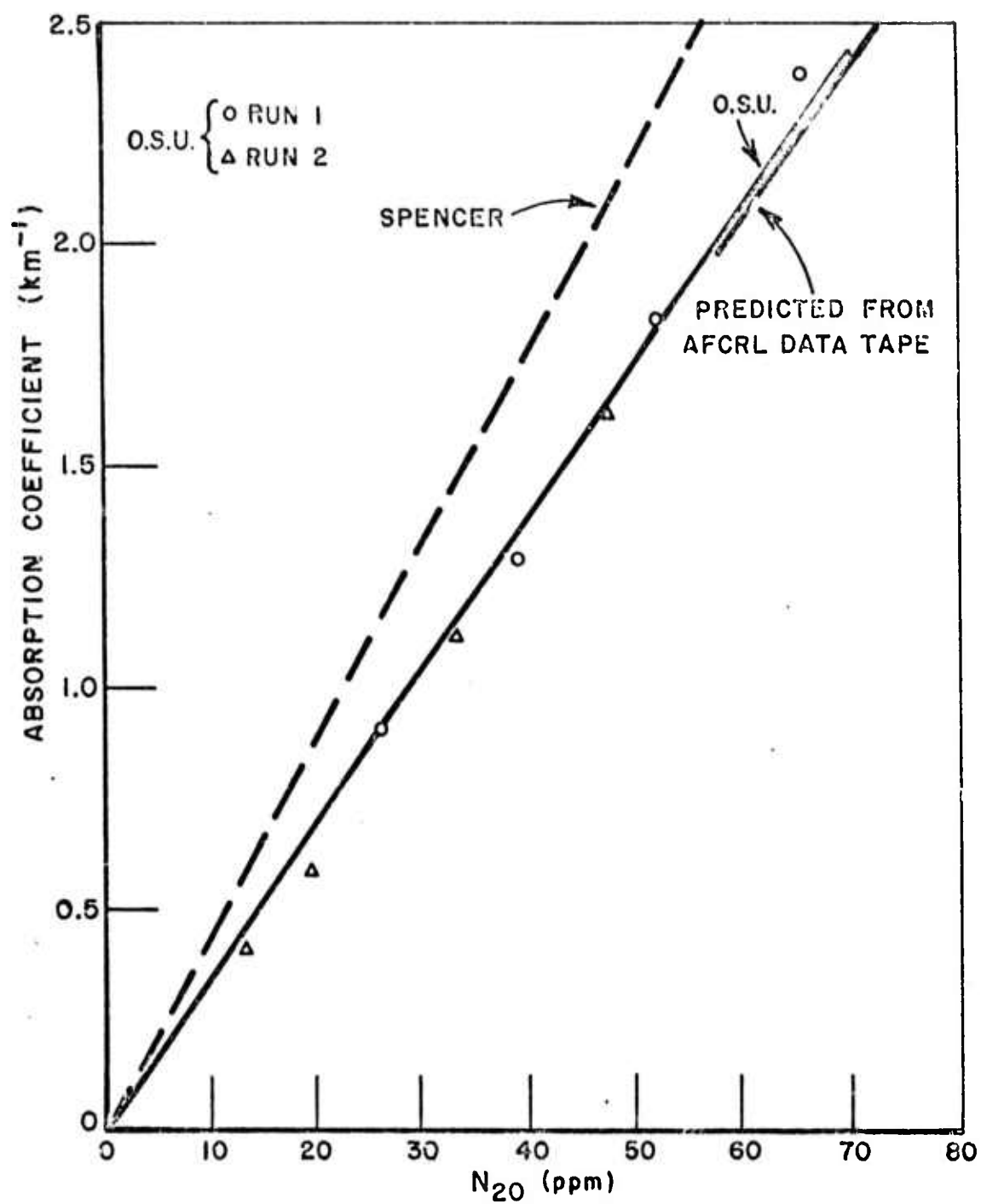Fig. 6. Measured N_2O-N_2 absorption coefficient for 2-1 P(10) line.

Fig. 7. Measured N_2O-N_2 absorption coefficient for 2-1 P(11) line.

11

Fig. 8. Calculated spectrum for 2545-2555 cm^{-1}.

12

ABSORBER: N2O
AMOUN (TORR): .0020
TEMP (DEG F): 72.00

03/01/74
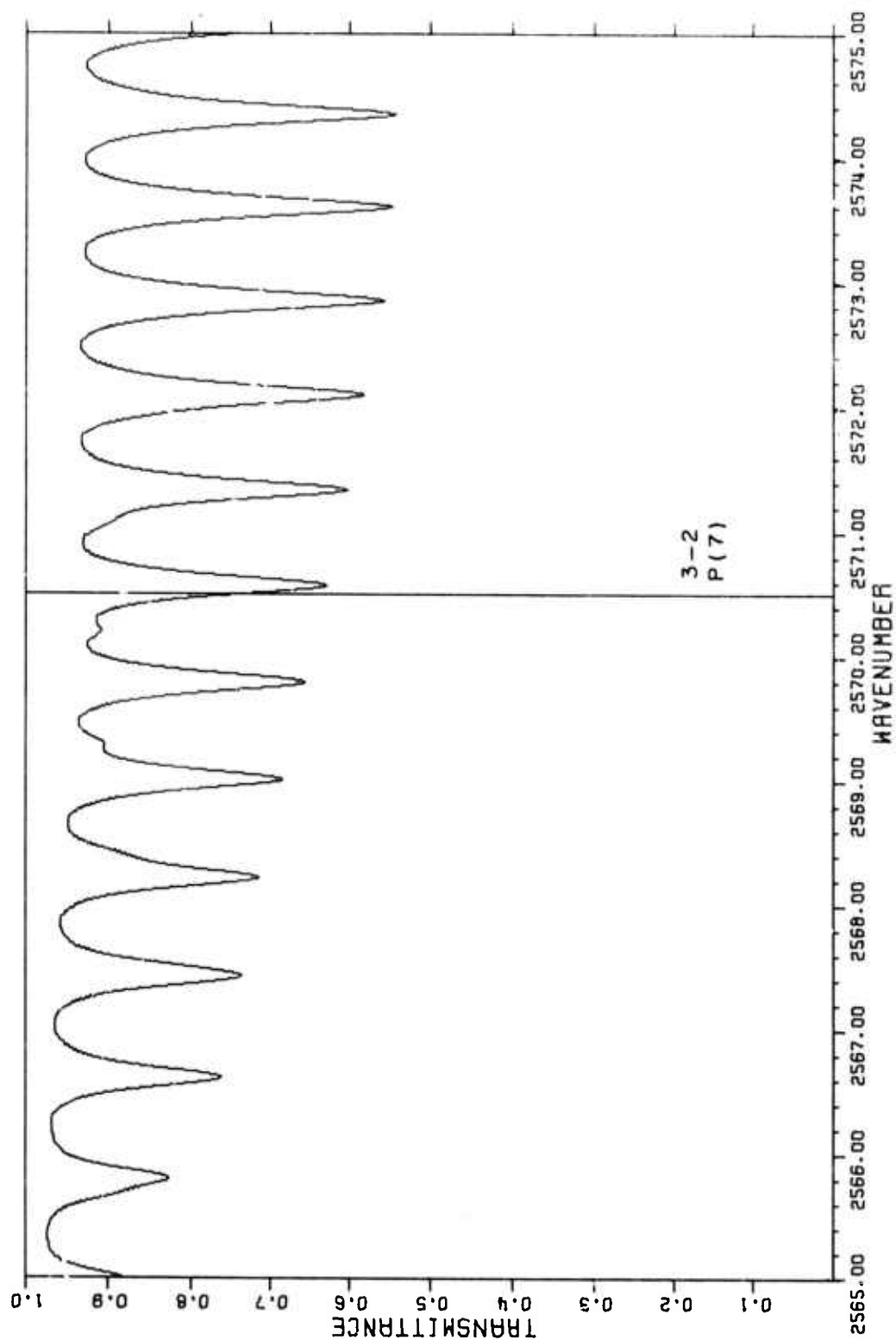TOTAL PRESSURE (TORR): 760.0
PATH LENGTH (METER): 1000.

3-2
P(7)

Fig. 9. Calculated spectrum for 2565-2575 cm^{-1}.

Fig. 10. Calculated spectrum for 2575-2585 cm^{-1}.

14

ABSORBER: N2O
AMOUNT (TORR): .0500
TEMP (DEG F): 72.00

03/11/74
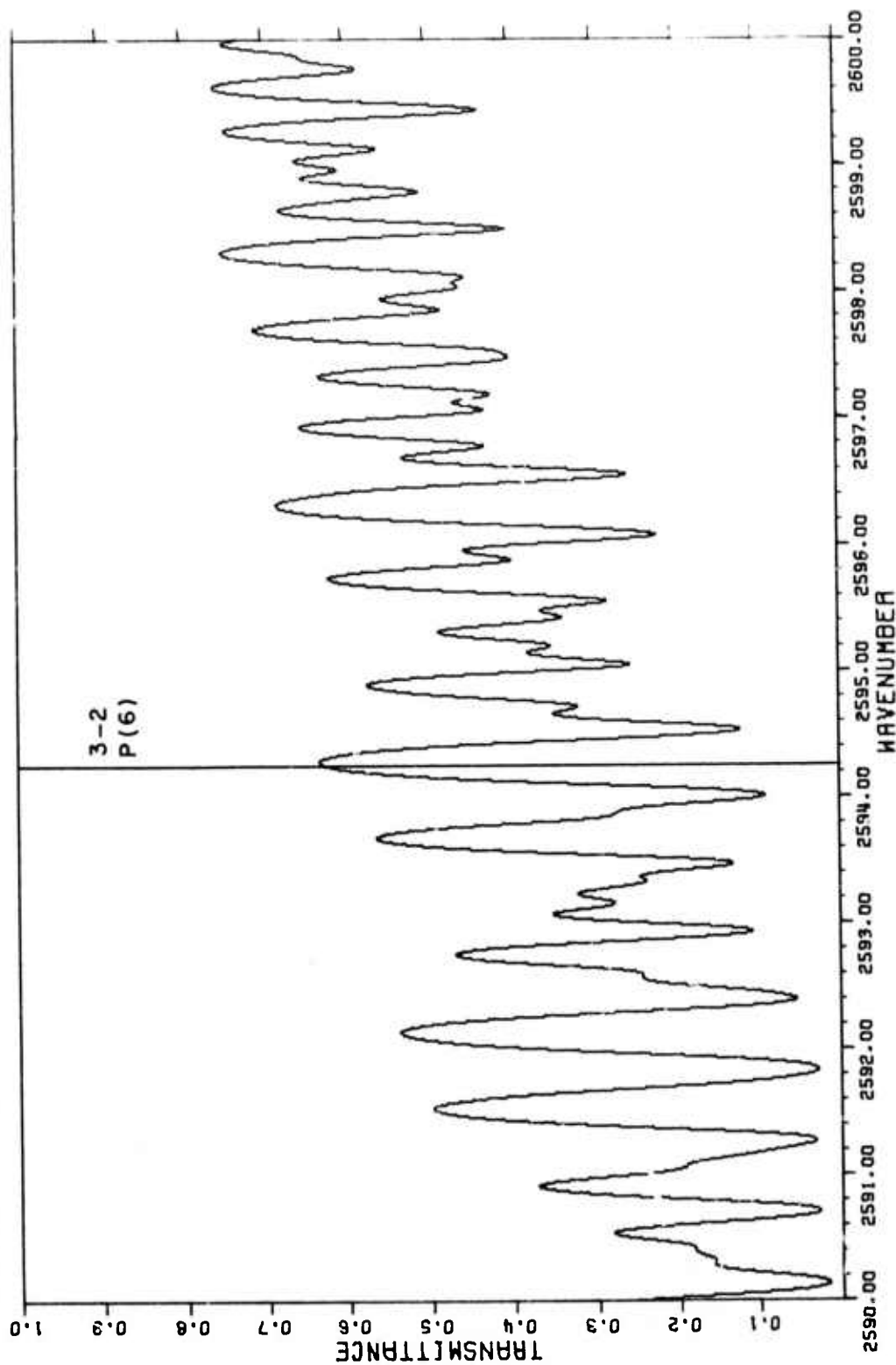TOTAL PRESSURE (TORR): 760.0
PATH LENGTH (METER): 1000.

Fig. 11. Calculated spectrum for 2590-2600 cm^{-1}.

15

IV. LINE SEPARATION EXPERIMENTS

For two of the laser lines, 3-2 P(7) and 2-1 P(10), the assumed laser frequency differs from the assumed frequency of an N_2O absorption line by less than one half-width. In this situation it is possible to obtain information about the separation of the laser line and absorption line by plotting the absorption coefficient as a function of total pressure with the absorber pressure constant.

This can be shown by the following [6]. For an isolated Lorentz line we have

$$(1) \qquad k = \frac{S}{\pi} \frac{\alpha}{(\Delta v)^2 + \alpha^2}$$

where k is the absorption coefficient,

$$\alpha = \alpha_0 \frac{P}{P_0} \left(\frac{T_0}{T} \right)^m$$

is the half-width of the absorption line, $P_0 = 1$ atm, Δv is the difference in the frequencies of the laser line and the absorption line, P is the total pressure and S is the line strength. For a constant temperature and P in atmospheres α becomes

$$\alpha = \alpha_0 P.$$

On a curve of k versus total pressure P the condition for zero slope with Δv constant is

$$(2) \qquad \frac{dk}{d\alpha} = \frac{S}{\pi} \left[\frac{(\Delta v)^2 + \alpha^2 - 2\alpha^2}{((\Delta v)^2 + \alpha^2)^2} \right] = 0$$

or,

$$(3) \qquad \alpha = \Delta v.$$

Therefore, as a first approximation (i.e., assuming a single isolated Lorentz line) the following expression holds:

$$(4) \qquad \alpha_0 P = \Delta v.$$

Thus, if the frequency difference between the laser line and the absorption line is accurately known, the half-width can be accurately determined. Similarly, if the half-width and frequency of the absorption line are accurately known, the laser frequency can be found.

16

In the present study, the laser frequencies were believed to be more uncertain than the half widths and frequencies of the N_2O absorption lines so the latter procedure was used to more accurately determine the laser frequencies.

It should be mentioned that Eq. (4) is strictly true only if the pressure is high enough that the Voigt profile does not have to be used to describe the absorption line shape, there is no pressure shift in the frequency of the absorption line, and there are no other absorption lines close enough to contribute to the absorption at the laser frequency. In the present study, the first two assumptions are valid, but the third one is not. It can be shown that the effect of considering other absorption lines which are close enough to contribute to the absorption at the laser frequency is to add a small positive term to the right hand side of Eq. (4). For the lines under consideration in the present study, the added term is 4 to 5 percent of Δv.

For the two lines studied, the experimental plot of absorption coefficient versus total pressure was used to make a first estimate of the laser frequency. Curves of absorption coefficient versus total pressure were calculated for several laser frequencies close to the estimated frequency using the AFCRL line data [4]. These calculated curves were then plotted along with the experimental data. The calculated curve which best fit the experimental data was then taken to represent the correct laser frequency.

Figure 12 shows the experimental data for the 3-2 P(7) line with N_2O pressure constant at 6.51×10^{-3} torr and total pressure varying from 50-850 torr along with calculated curves for the same N_2O pressure and laser frequencies 2570.505 cm^{-1}, 2570.510 cm^{-1}, and 2570.515 cm^{-1}. The laser frequency determined from Fig. 12 is $2570.51 \pm .01$ cm^{-1}.

Figures 13 and 14 show the experimental data for the 2-1 P(10) line with N_2O pressures 6.82×10^{-3} torr and 1.73×10^{-2} torr respectively and total pressure from 50 torr to 760 torr. Also shown are calculated curves for the same N_2O pressures and laser frequencies 2580.100 cm^{-1}, 2580.105 cm^{-1}, and 2580.110 cm^{-1}. The laser frequency determined from the plots is $2580.10 \pm .005$ cm^{-1}. This is in agreement with the frequency calculated from molecular constants [7].
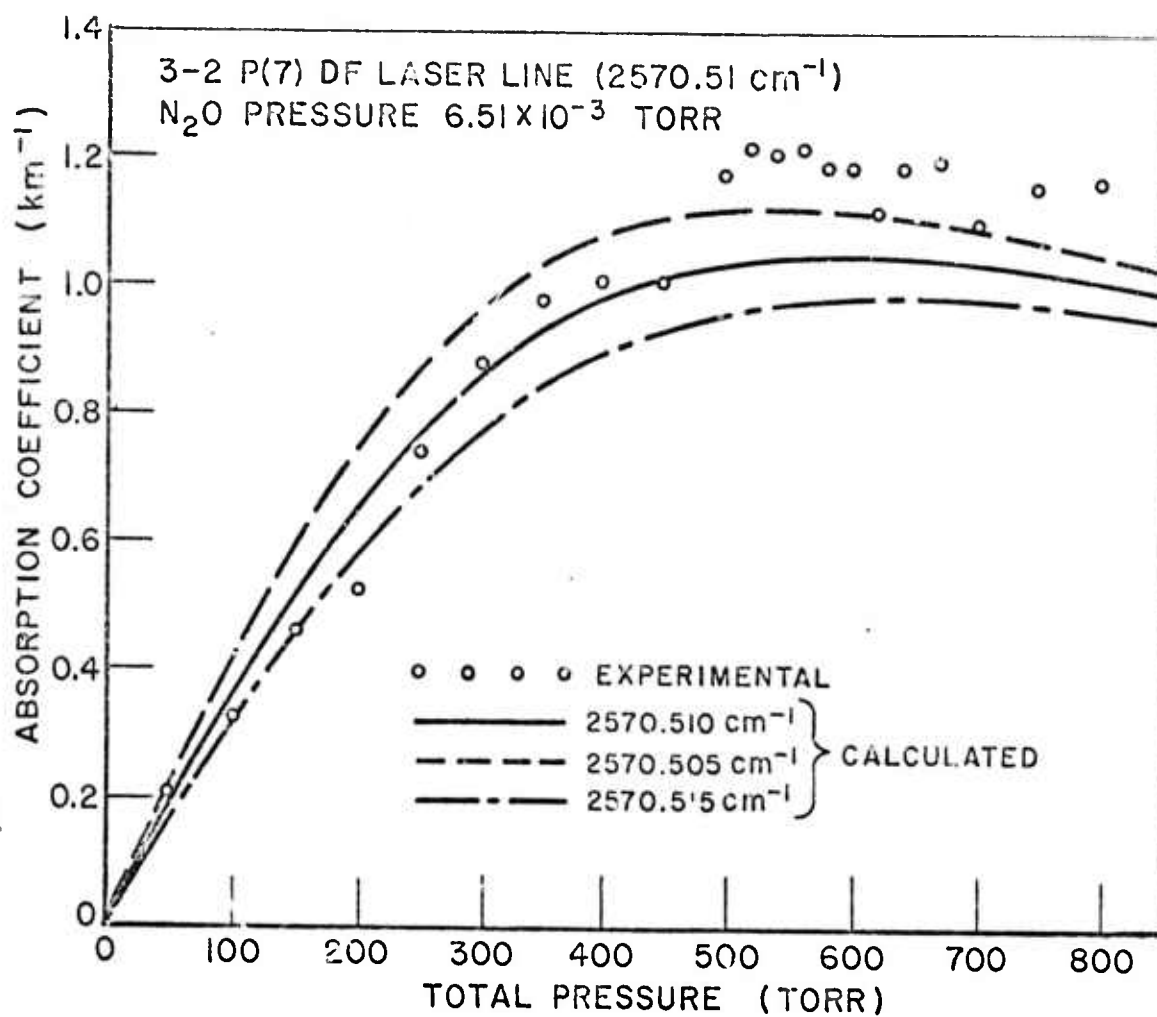
17

Fig. 12.   Absorption coefficient vs total pressure for 3-2 P(7) line
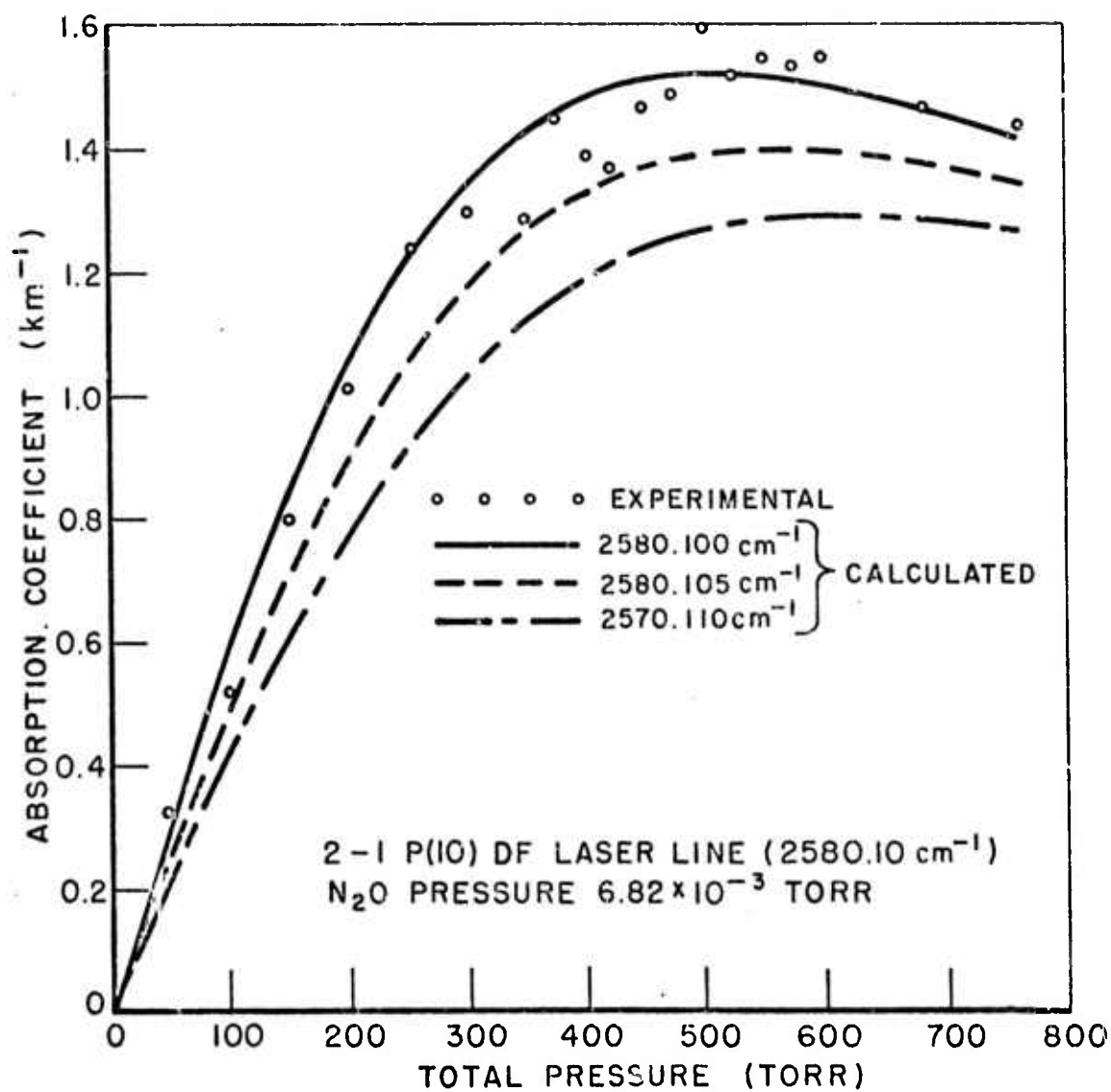at 6.51 x 10⁻³ torr N₂O.

18

Fig. 13. Absorption coefficient vs total pressure for 2-1 P(10) line
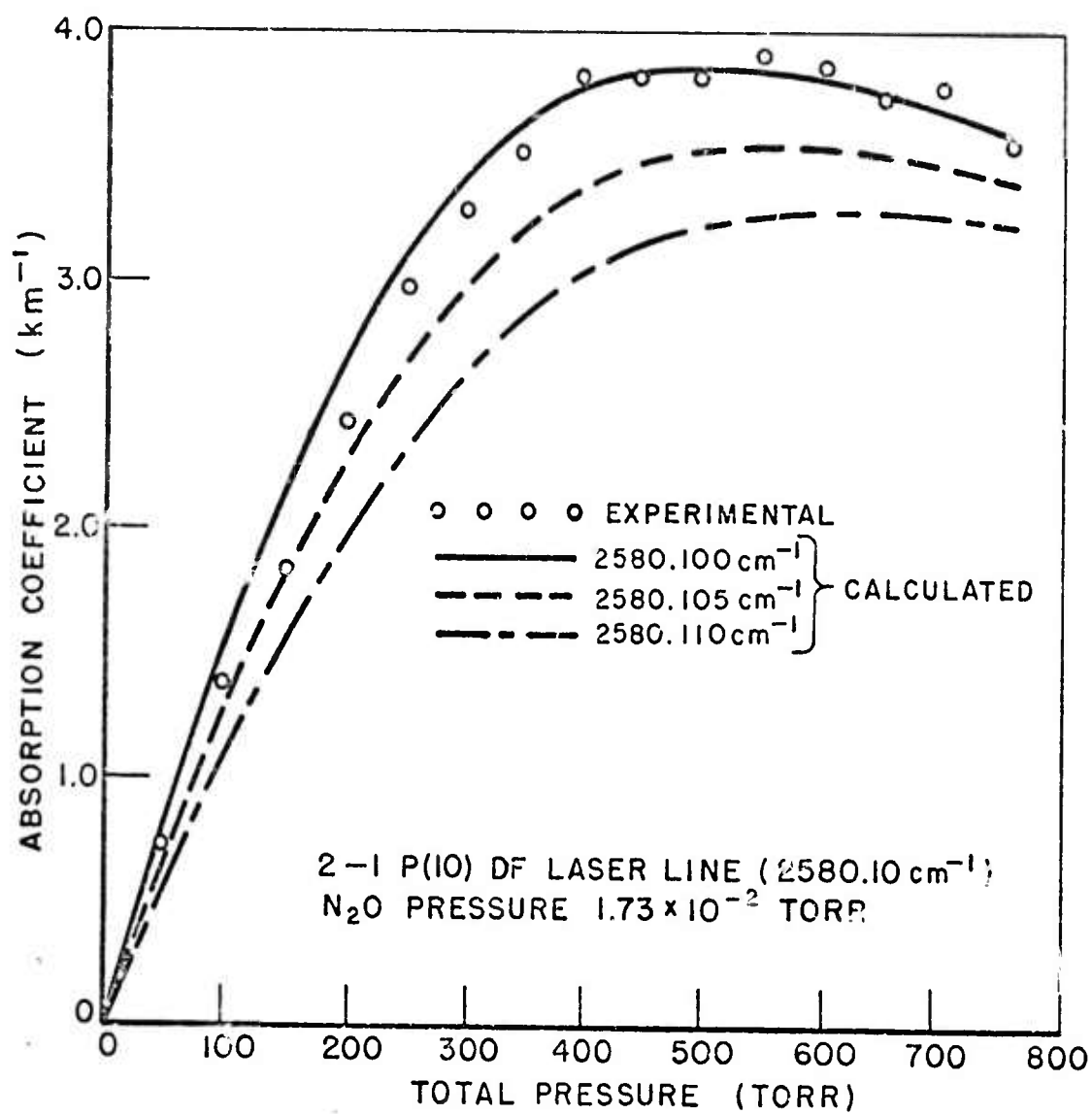at 6.82×10^{-3} torr N_2O.

Fig. 14. Absorption coefficient vs total pressure for 2-1 P(10) line at 1.73 x 10⁻² torr N₂O.

V. CONCLUSIONS

The measurements presented in this report confirm the previously
available experimental work and the calculations based on the AFCRL
line data tape. Better DF laser frequency data is needed especially
for the 3-2 band.

Techniques developed during this investigation are applicable to
the water vapor absorption studies which are now underway. This in-
cludes the laser, detector calibration, data integration and recording
system, etc.

21

APPENDIX A
DETECTOR LINEARITY CALIBRATION

The detectors used in these measurements are room temperature lead selenide photo conductive detectors. The rise time of these detectors is about 1 microsecond so that they are fast enough to respond to the peak power of the laser rather than average power. Although the average power is only on the order of 1 milliwatt, the peak power is about 100 watts. The detectors are definitely non-linear in this region so they must be calibrated for linearity.

The lead selenide detectors were calibrated against an Eppley thermopile which has about a 1 second response time, and therefore measures average power rather than peak power. The thermopile is known to be linear in this range.

The laser line used for calibration was the 3-2 P(7) line since it was one of the lines of interest and it could be easily attenuated using a small absorption cell filled with various amounts of N_2O. The calibration should also be good for other lines, although this assumption will need to be tested.

The experimental layout for the calibration experiment is shown in Fig. 1 of the main report. The experiment was done in two parts. For the first part of the experiment, mirror M2 was installed and detector #1 was compared with the thermopile over a wide range of signal levels. The laser was adjusted for optimum operation on the 3-2 P(7) line, and then left undisturbed for the remainder of the ex-periment. The signal amplitude at the detectors was lowered step by step by introducing N_2O into the 21 cm cell. At each step the signals from detector #1 and the Eppley thermopile were read and recorded on the typewriter by the computer. This part of the experiment was repeated three times on three separate days. For the second part of the experiment mirror M2 was removed and detector #1 and detector #2 were compared.

A least squares fit of the data from the first part of the experiment was made to a third order polynomial. This yields an expression of the form

$$(5) \qquad E_1 = A_0 + A_1 X_1 + A_2 X_1^2 + A_3 X_1^3$$

relating PbSe detector #1 signal to Eppley thermopile signal where X_1 corresponds to PbSe #1 signal and E corresponds to Eppley signal (Fig. 15). Similarly the data from the second part of the experi-ment was used to obtain an expression of the form

$$(6) \qquad X_1 = C_0 + C_1 X_2 + C_2 X_2^2 + C_3 X_2^3 \ .$$
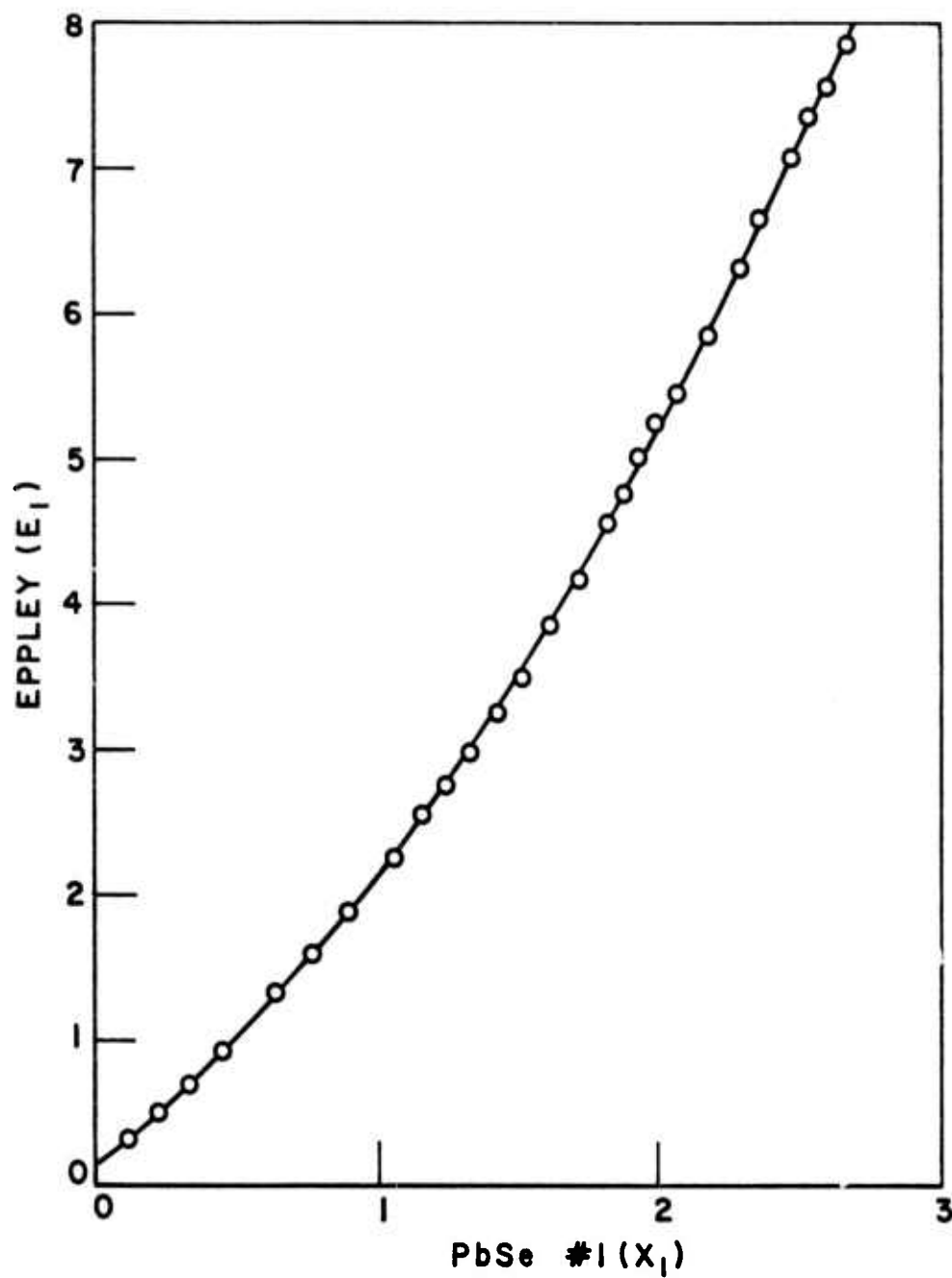
23

Fig. 15. Eppley thermopile detector calibration signal versus lead selenide detector number one. Units are volts at A/D converter after arbitrary amplifications.

24

Where X_2 corresponds to PbSe #2 signal and X_1 corresponds to PbSe #1 signal (Fig. 16). From Eqs. (5) and (6) it is now possible to determine the following expression relating PbSe #2 signal, X_2, to Eppley signal, E_2 (Fig. 17).

$$(7) \qquad E_2 = B_0 + B_1 X_2 + B_2 X_2^2 + B_3 X_2^3$$

The calibration was tested by putting Eqs. (5) and (7) in the data taking program and repeating the second part of the calibrating experiment. Figure 18 shows the result of that experiment. If the linearity calibration is good, the data should fall on a straight line through the origin. Figure 18 shows that this is very nearly true. A second check on the calibration is the actual absorption data (Figs. 3-7). Since the data falls on a straight line, this is a second indication that the calibration is good. For low absorber partial pressures, the absorption data is in fact the best check on calibration.
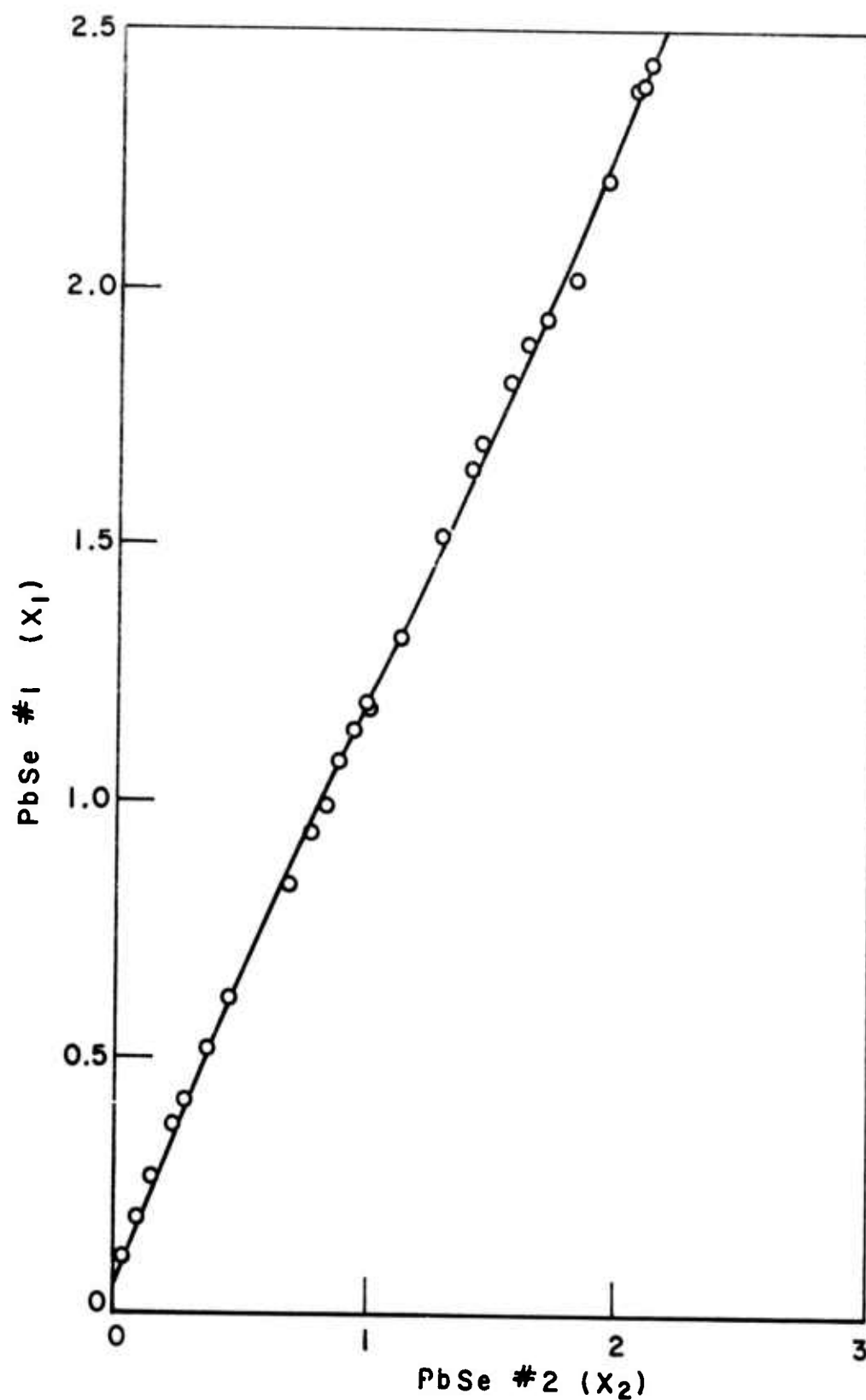
Fig. 16. Calibration of lead selenide detector #2 in terms of lead selenide detector #1. Units are volts at A/D converter after arbitrary amplifications.
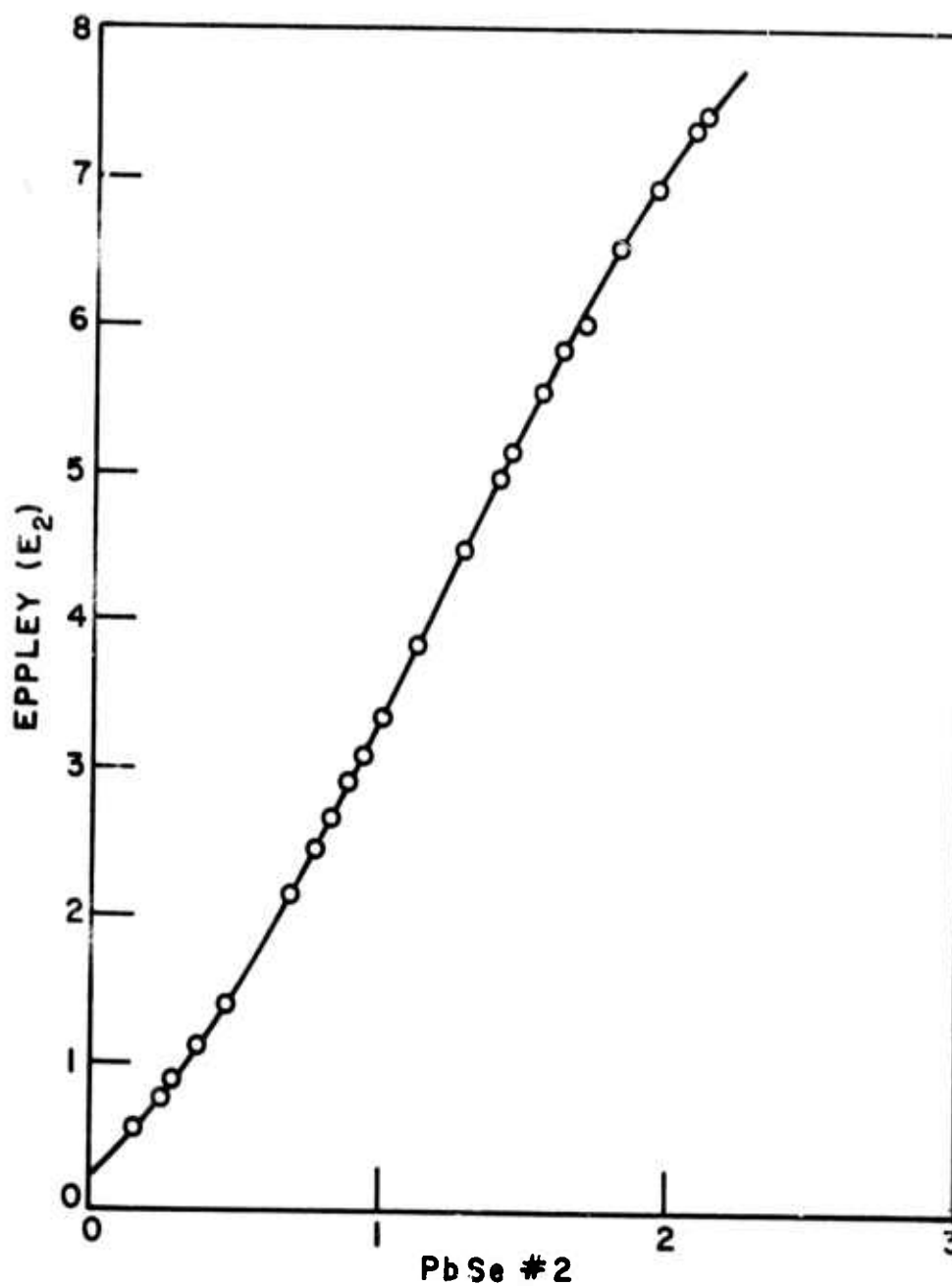
26

Fig. 17. Derived curve relating PbSe #2 detector to Eppley thermopile. Units are volts at A/D converter after arbitrary amplifications.
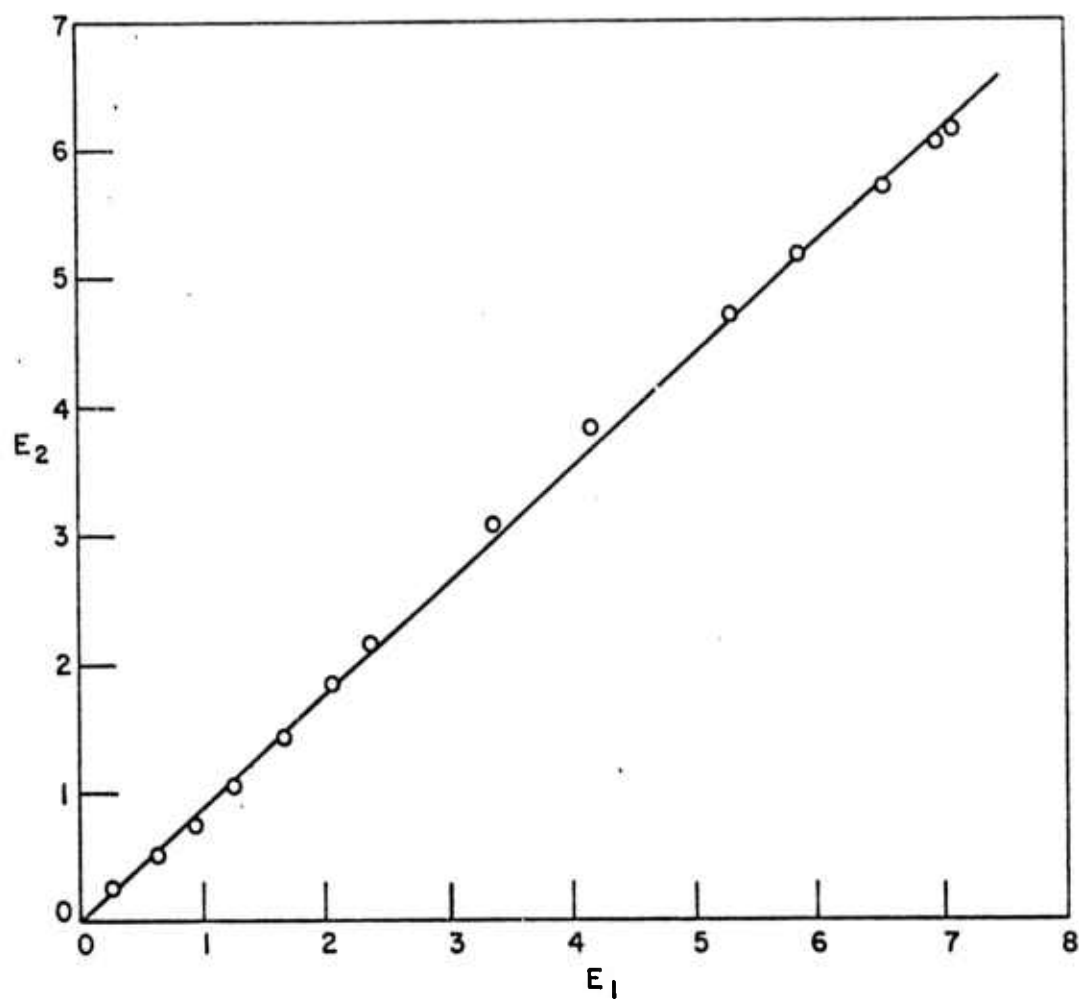
Fig. 18.   Linearity curve derived from data
in Figs. 15 and 16.   Relative units.

MISSION
of
Rome Air Development Center

RADC is the principal AFSC organization charged with
planning and executing the USAF exploratory and advanced
development programs for electromagnetic intelligence
techniques, reliability and compatibility techniques for
electronic systems, electromagnetic transmission and
reception, ground based surveillance, ground
communications, information displays and information
processing. This Center provides technical or
management assistance in support of studies, analyses,
development planning activities, acquisition, test,
evaluation, modification, and operation of aerospace
systems and related equipment.